W-band Polarimetric Scattering Features of a Tactical Ground Target Using a 1.56THz 3D Imaging Compact Range

Daniel R. Culkin, Guy B. DeMartinis, Thomas M. Goyette, Jason C. Dickinson,
and Jerry Waldman
Submillimeter Wave Technology Laboratory
University of Massachusetts Lowell, 175 Cabot Street, Lowell, MA 01854

And

William E. Nixon
U.S. Army National Ground Intelligence Center
220 Seventh Street, N.E., Charlottesville, VA 22902

ABSTRACT

In this study the polarization scattering matrices (PSM) of individual scatterers from a complex tactical ground target were measured as a function of look angle. Due to the potential value of PSMs in studies of automatic target recognition, a fully polarimetric, three-dimensional spot scanning radar modeling system was developed at 1.56 THz to study the W-band scattering feature behavior from 1/16th scale models of targets. Scattering centers are isolated and coherently measured to determine the PSMs. Scatterers of varying complexity from a tactical target were measured and analyzed, including well-defined fundamental odd and even bounce scatterers that maintain the exact normalized PSM with varied look angle, scatterers with varying cross- and co-pol terms, and combination scatterers. Maps defining the behavior of the position and PSM activity over varying look angle are likely to be unique to each target and could possibly represent exploitable features for ATR.

The high-resolution spot scanning radar system transceiver uses a high-stability, narrow-band optically pumped far infrared laser and implements laser/microwave sideband generation. The measurement system is a heterodyned, fully polarimetric, three-dimensional imaging system, using raster scanning and frequency chirping to obtain the 3D image. The effect of mapping the 3D polarimetric scattering center data into range/cross-range ISAR imagery is demonstrated. The mapping showed considerable promise for retaining consistency over varying look angles, and the corresponding ISAR imagery demonstrated similar characteristics. The results were then analyzed in linear polarization and circular polarization bases for possible manipulations for the purpose of a simple ATR. A method utilizing the properties of two circular polarization receive states is demonstrated and its performance analyzed.

1. Introduction

The Submillimeter Wave Technology Laboratory (STL) at UMass Lowell has developed several compact radar ranges, and in recent years has updated these ranges to have fully polarimetric capabilities. Polarimetric data contains all possible information available about a scatterer/target for a given resolution, an obvious advantage over more common single pol data in studies of target behavior and ATR. In order to realize that potential the polarimetric behavior of individual scatterers over varying look angles must be carefully measured and analyzed.

Analysis of the polarimetric behavior of scatterers taken on a T80 tank by a three-dimensional imaging system (3DI) has shown that the normalized polarization scattering matrices remain virtually identical over a modest change in look angle ($\pm 5^{\circ}$). These 3DI images were then projected into a top-view form, giving a spot-scanned "ISAR", and compared to actual ISAR data of the same resolution. While there are differences in the amplitudes of scatterers (due primarily to elevation related phasing and aperture dependent pixel division) the PSMs of the ISAR images show similar behavior to the spot scanned 3DI top view.

Both linear and circular polarization bases (LP and CP, respectively) were then considered for use in the creation of a simple target recognizer algorithm. The combination of odd/even bounce scatterer segregation coupled with the

Algorithms for Synthetic Aperture Radar Imagery VIII, Edmund G. Zelnio, Editor,
Proceedings of SPIE Vol. 4382 (2001) © 2001 SPIE · 0277-786X/01/$15.00

Report Documentation Page

Form Approved
OMB No. 0704-0188

Public reporting burden for the collection of information is estimated to average 1 hour per response, including the time for reviewing instructions, searching existing data sources, gathering and maintaining the data needed, and completing and reviewing the collection of information. Send comments regarding this burden estimate or any other aspect of this collection of information, including suggestions for reducing this burden, to Washington Headquarters Services, Directorate for Information Operations and Reports, 1215 Jefferson Davis Highway, Suite 1204, Arlington VA 22202-4302. Respondents should be aware that notwithstanding any other provision of law, no person shall be subject to a penalty for failing to comply with a collection of information if it does not display a currently valid OMB control number.

1. REPORT DATE	2. REPORT TYPE	3. DATES COVERED
AUG 2001		**00-00-2001 to 00-00-2001**

4. TITLE AND SUBTITLE	5a. CONTRACT NUMBER
W-band Polarimetric Scattering Features of a Tactical Ground Target Using a 1.56THz 3D Imaging Compact Range	5b. GRANT NUMBER
	5c. PROGRAM ELEMENT NUMBER
6. AUTHOR(S)	5d. PROJECT NUMBER
	5e. TASK NUMBER
	5f. WORK UNIT NUMBER
7. PERFORMING ORGANIZATION NAME(S) AND ADDRESS(ES) **University of Massachusetts Lowell,Submillimeter-Wave Technology Laboratory,175 Cabot Street,Lowell,MA,01854**	8. PERFORMING ORGANIZATION REPORT NUMBER
9. SPONSORING/MONITORING AGENCY NAME(S) AND ADDRESS(ES)	10. SPONSOR/MONITOR'S ACRONYM(S)
	11. SPONSOR/MONITOR'S REPORT NUMBER(S)

12. DISTRIBUTION/AVAILABILITY STATEMENT
Approved for public release; distribution unlimited

13. SUPPLEMENTARY NOTES

14. ABSTRACT

15. SUBJECT TERMS

16. SECURITY CLASSIFICATION OF:			17. LIMITATION OF ABSTRACT	18. NUMBER OF PAGES	19a. NAME OF RESPONSIBLE PERSON
a. REPORT **unclassified**	b. ABSTRACT **unclassified**	c. THIS PAGE **unclassified**		**11**	

unsegregated odd/even appearance of noise, clutter, and unresolvable random scattering pointed to a CP basis having an inherent advantage. A simple manipulation creating polarization based images is demonstrated, and is compared to the performance of similar single pol LP and CP procedures.

2. The 3DI Compact Range Description and Data Analysis

The STL 3DI compact range is described in detail in ref [1, 2]. It is a spot scanning, fully polarimetric system operating at 1.56THz, with a bandwidth of 7GHz. The 1.56THz source consists of two CO_2-laser-pumped far infrared lasers using difluoromethane (CH_2F_2) and the laser cavity lengths tuned to generate a frequency difference of 1MHz. The transmitter and vertical and horizontal polarization receivers are corner-cube-mounted Schottky diodes. The transmit polarization can be rotated by means of a motorized polarizer, hence only vertical (V) or horizontal (H) linear polarization states (with respect to the ground plane) can be transmitted at a time. Simultaneous reception of V and H is performed using a wire grid polarizer and two receivers.

The transmitter Schottky diode mixes the base laser frequency with a microwave generator frequency to produce a sideband, shifted 10-17 GHz from the base 1.56THz. The polarization of the resulting sideband frequency is optimized and the radiation is guided to a large focusing mirror, focusing the radiation to a 1 centimeter gaussian spot in the target zone. Using a 6 axis motorized stage, the target is then translated horizontally with data points being oversampled by a factor of 3 with respect to the focused beam spot size. The transmit polarization is then rotated and the process repeated for the orthogonal transmit pol. Once the image is created, scatterers can be isolated in volume and their polarization scattering matrices (PSMs) can be determined. A sample 3D image is shown in Figure 1.

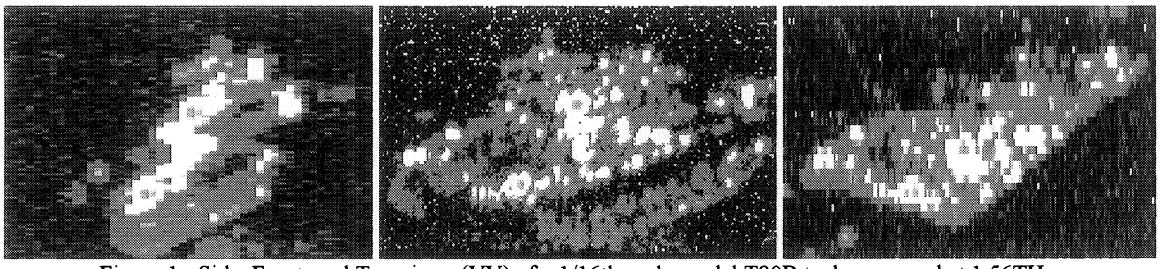

Figure 1: Side, Front, and Top views (VV) of a 1/16th scale model T80B tank measured at 1.56THz.

Measurements were taken on a 1/16th scale model of a T80B tank. At 1/16th scale, the compact range models W-band radar (90-100 GHz). The PSMs of several different types of scatterers are described as a function of look angle in Tables 1a , 1b, and 1c.

$$\begin{pmatrix} HH < phase & VH < phase \\ HV < phase & VV < 0^\circ (ref.) \end{pmatrix} (dBsm)$$

$\begin{bmatrix} 10^\circ elevation \\ 25^\circ aspect \end{bmatrix}$	$\begin{bmatrix} 10^\circ elevation \\ 30^\circ aspect \end{bmatrix}$	$\begin{bmatrix} 10^\circ elevation \\ 35^\circ aspect \end{bmatrix}$
$\begin{bmatrix} 15^\circ elevation \\ 25^\circ aspect \end{bmatrix}$	$\begin{bmatrix} 15^\circ elevation \\ 30^\circ aspect \end{bmatrix}$	$\begin{bmatrix} 15^\circ elevation \\ 35^\circ aspect \end{bmatrix}$
$\begin{bmatrix} 20^\circ elevation \\ 25^\circ aspect \end{bmatrix}$	$\begin{bmatrix} 20^\circ elevation \\ 30^\circ aspect \end{bmatrix}$	$\begin{bmatrix} 20^\circ elevation \\ 35^\circ aspect \end{bmatrix}$

Table 1a: The look angles corresponding to the matrix placement of the PSMs shown in tables 1b and 1c.

$\begin{pmatrix} 14.0 < 12^\circ & -- \\ -- & 12.6 < 0^\circ \end{pmatrix}$	$\begin{pmatrix} 13.0 < 14^\circ & -- \\ -- & 13.6 < 0^\circ \end{pmatrix}$	$\begin{pmatrix} 15.3 < 9^\circ & -- \\ -- & 14.8 < 0^\circ \end{pmatrix}$
$\begin{pmatrix} 16.7 < 0^\circ & -- \\ -- & 16.8 < 0^\circ \end{pmatrix}$	$\begin{pmatrix} 15.2 < -15^\circ & -- \\ -- & 14.6 < 0^\circ \end{pmatrix}$	$\begin{pmatrix} 15.7 < -9^\circ & -- \\ -- & 15.0 < 0^\circ \end{pmatrix}$
$\begin{pmatrix} 14.0 < 25^\circ & -- \\ -- & 14.3 < 0^\circ \end{pmatrix}$	$\begin{pmatrix} 11.1 < 27^\circ & -11.4 < -61^\circ \\ -12.7 < 3^\circ & 11.6 < 0^\circ \end{pmatrix}$	$\begin{pmatrix} 16.8 < 42^\circ & -12.4 < -120^\circ \\ -12.4 < -120^\circ & 17.8 < 0^\circ \end{pmatrix}$

$\begin{pmatrix} 6.8 < 161^\circ & -- \\ -- & 9.5 < 0^\circ \end{pmatrix}$	$\begin{pmatrix} 7.3 < 161^\circ & -- \\ -- & 9.9 < 0^\circ \end{pmatrix}$	$\begin{pmatrix} 5.0 < -170^\circ & -- \\ -- & 11.1 < 0^\circ \end{pmatrix}$
$\begin{pmatrix} 9.8 < 174^\circ & -- \\ -- & 10.2 < 0^\circ \end{pmatrix}$	$\begin{pmatrix} 8.0 < 176^\circ & -- \\ -- & 7.4 < 0^\circ \end{pmatrix}$	$\begin{pmatrix} 13.0 < 177^\circ & -- \\ -- & 13.1 < 0^\circ \end{pmatrix}$
$\begin{pmatrix} 13.6 < 158^\circ & -- \\ -- & 12.5 < 0^\circ \end{pmatrix}$	$\begin{pmatrix} 4.3 < 127^\circ & -- \\ -- & 5.4 < 0^\circ \end{pmatrix}$	$\begin{pmatrix} 13.3 < -159.6^\circ & -- \\ -- & 14.9 < 0^\circ \end{pmatrix}$

Tables 1a and 1b: On the left, the PSMs of a bright "odd bounce" scatterer, and on the right the PSMs of a bright "even bounce" scatterer.

While the actual values of the PSMs may be varying over this ten degree by ten degree swath of look angles, the normalized nature of the PSMs remains fairly constant. This is an important item since a rapidly varying PSM would undermine a key ingredient of using polarimetric data for ATR - that minor changes in incident radiation angle would not preserve the polarimetric behavior of a scattering center.

3. Spot Scan Versus ISAR Comparison

While the spot scanning method creates a very accurate portrayal of the complete assembly of scatterers that make up a target, it is not a practice that can be applied to field imaging. Two major differences between spot scanned and ISAR data are the phasing issues that occur with ISAR imaging, and that an ISAR image contains information from the target over a range of look angles.

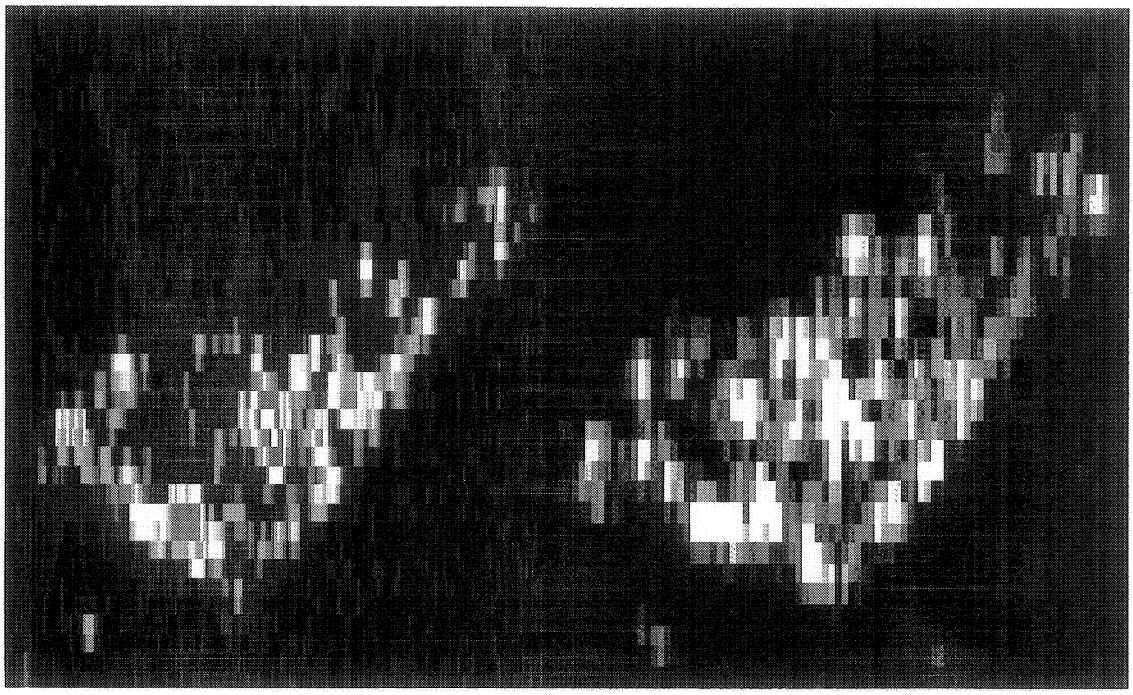

Figures 2a and 2b: A T80B tank at 15° elevation, 30° aspect. The image on the left is a top view of the tank measured on the spot scanning 3DI system, the image on the right is an ISAR image (different resolutions).

While these are significant differences, they do not change the implication of the 3DI system study - that the behavior of the normalized PSM remains virtually unchanged over look angle, even when the scatterers are compressed into two dimensions. A VV comparison of the 3DI data taken on a T80B with the ISAR data is shown in Figure 2. Figure 2a is an image made by projecting the 3D data onto a top view of the target. Figure 2b is an ISAR data set taken at the same angle. The ISAR measurements were made in a separate 1.56 THz compact range where the model target is fully illuminated by the radar beam. The target is mounted on a pylon, rotated in azimuth and the coherent data is processed by a two dimensional FFT to produce conventional ISAR imagery. A complete description of this range is provided in a separate paper (ref. [3, 4]).

4. Polarimetric ISAR and Basis Selection

Although the measurements in this study have been taken in linear polarization coordinates (LP), there is value to converting the data to circular polarization coordinates (CP). In LP, the intensity images created do not contain the relative phase information between the channels the way in which CP does, which is important for segregating types of scatterers. In general, CP distinguishes scatterer descriptions into odd bounce (cross-pols) and even bounce (co-pols) channels. Since for most targets the TRCS comes from geometries that return predominantly even or odd bounce scattering, use of the co- and cross-pol CP channels shows the most promise for ATR use.

5. Polarimetric ATR Study

5.1 Technique for Image comparison

In order to demonstrate the value of polarimetric ATR and use of different coordinate systems, a simple algorithm was developed to assign numerical scores to test images when compared to a template image. The algorithm consists of creating images every one degree from 0°-360° in aspect for all data sets at near identical resolutions. One image is selected from a data set to be used as a template image, and is compared to the 361 images of another data set (test images), with scores being determined for each image. The numerical score of the comparison is calculated by subtracting each pixel amplitude in the test image from its corresponding pixel amplitude in the template image. The value of pixels in the remaining difference image are added, and that number divided by the sum of the values in all pixels of both original images #1(template) and #2 (test). One minus that number times 100 gives the score in percent with 100% being a perfect match and 0% being the worst possible match (see Equations 1a and 1b). In order to ensure the spatial alignment of the images, a self-registration algorithm has been implemented. It translates the test image over a controlled square of positions, with the position giving the maximum score being considered the correct alignment position.

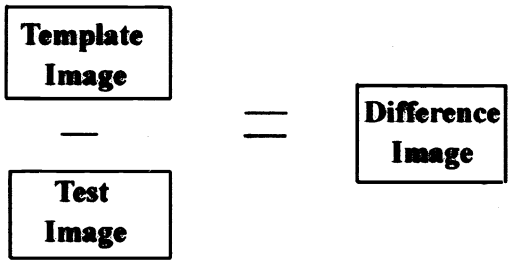

$$(Template)_{ij} - (Test)_{ij} = (Difference)_{ij} \qquad \text{(Equation 1a)}$$

$$Score\% = \{1 - \sum_{i,j} |Difference| \Big/ [\sum_{i,j} |Template| + \sum_{i,j} |Test|]\} \times 100 \qquad \text{(Equation 1b)}$$

Data sets for W-band and Ka-band ISAR that were used in this study were measured from 1/16th scale models of tactical targets. Since the data is fully polarimetric, it can be processed into ISAR images (range and crossrange) in either the LP or the CP basis. Three studies were done using the different polarization coordinates in order to determine the benefits of each. Using the numerical techniques described above, linearly polarized images (VV), circularly polarized images (RR), then newly developed 2 channel CP images (described below) were created and cross-correlated.

5.2 Image Construction

The images to be compared are constructed in several steps - The initial step is to define an "image separation threshold", a level in amplitude in which all signals weaker than a specified value can be considered insignificant. The pixel values of all images are compared to the image separation threshold in logarithmic space (dBsm). Any pixel from which the value is less than the image separation threshold is replaced by the value of the image separation threshold. For the two channel CP method, the RL image is subtracted from the corresponding RR image in logarithmic space (corresponding to a ratio in linear space). This gives a single new image that can be analyzed using the technique of section 5.1 for the single channel LP and CP method

The images to be compared in the VV and RR studies will only have positive values and zero values. The two channel method contains positive or negative values, depending on the "oddness" or "evenness" of the corresponding pixels. For example, a pixel that has a higher value in RR, the even bounce channel, than it does in RL, the odd bounce channel, will result in a positive pixel with an amplitude corresponding to the "evenness", or ratio of polarimetric preference.

The use of the 2CP method has several advantages over the single channel methods. Complex or random scattering in a linear basis will generally yield comparable amplitudes in the VV and HH channels, but with a random relative phase. This random relative phase equates to equal amplitudes in the even and odd bounce channels in a CP basis, which will be

subtracted out when using the 2CP method, whereas in a single channel basis the "noise" must be considered as a true feature of the target. This phenomenon applies to multiple unresolvable small scatterers, defects (scratches, small dents, etc.), and mixed scatterers of different elevation but the same range and cross range. The 2CP method will be more dependent on the actual characteristics of the scattering centers on the target and reduce the positive correlation score resulting from the coincidence of spatial alignment of the template and test images. Figures 3 and 4 show examples of typical images of targets as displayed in VV and 2 channel CP.

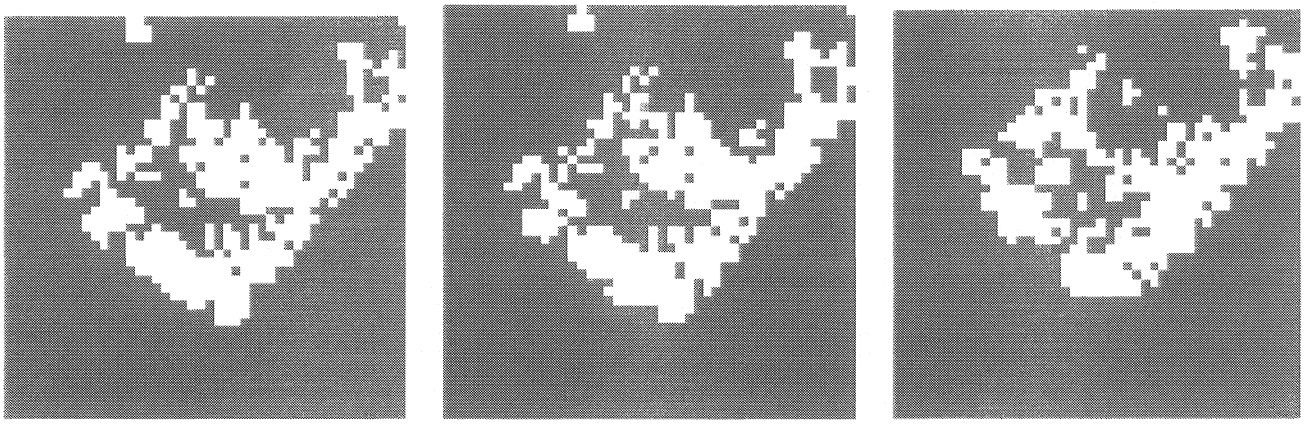

Figure 3: VV ISAR images of (from left to right) a T72M1, another measurement of a T72M1, and a T80U, 5° elevation, 220° aspect. A white pixel merely represents a VV amplitude above a -25dBsm threshold.

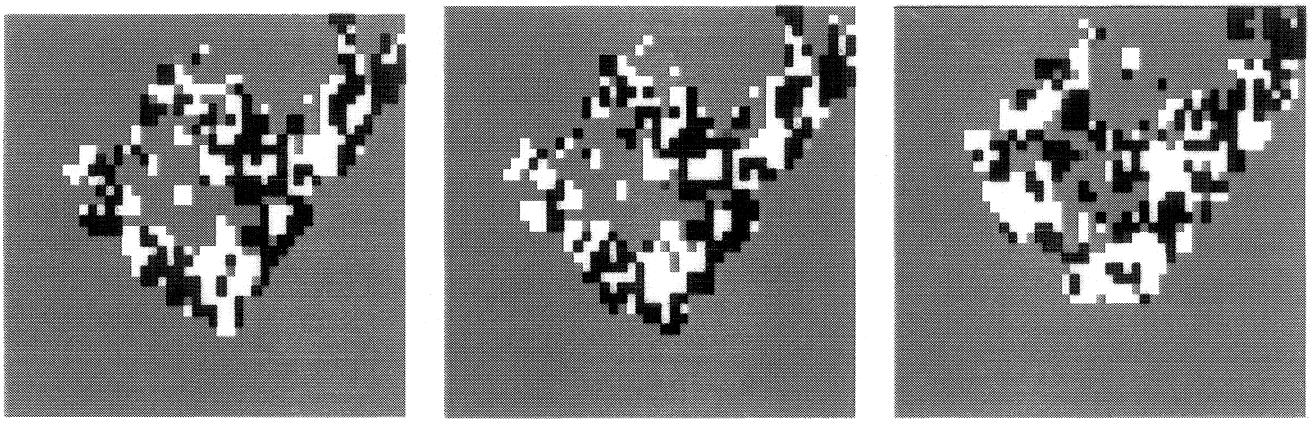

Figure 4: 2CP ISAR images of (from left to right) a T72M1, another measurement of a T72M1, and a T80U, 5° elevation, 220° aspect. A white pixel represents a pixel that displays "evenness", and a black pixel represents a pixel that displays "oddness".

In the VV images, the T80U image appears to be very similar to the T72M1s, possibly creating a situation where a correlation could generate a false alarm. The 2CP method produces very similar images for the T72 M1 measurements but a considerably different T80U image.

6. Results

6.1 Correlation Graphs

A systematic study was done using two collections of ISAR data - 12 sets of scale model W-band data taken at the STL, and 10 sets of scale model Ka-band data taken at NGIC. The data sets include many varieties of combinations of models and configurations. The comparisons are plotted as score (vertical axis) versus test image aspect angle (horizontal axis).

The data shown in Figure 5 demonstrates a typical correlation graph of images generated in VV. In this example the data is taken in Ka-band, though the same behavior is typical in W-band data. The template image is a T72Bk tank at 45° aspect, 5° elevation, and is being compared to another data run of the same tank at the same elevation angle.

Figure 5: T72Bk vs. T72Bk, LP basis (VV), Ka-band.

Figure 6: T72Bk vs. T72Bk, CP basis (RR), Ka-band.

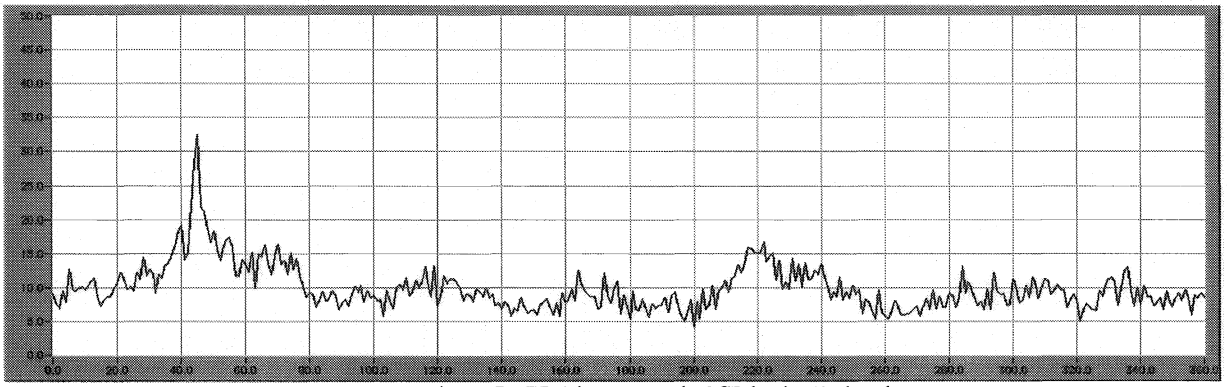

Figure 7: T72Bk vs. T72Bk, 2CP basis, Ka-band.

When the VV result is compared to the RR result (Figure 6) produced with the same data the method appears to show no significant advantage to using a CP basis over an LP basis. While the VV and RR correlation plots show a peak match at the proper 45° aspect angle, when compared to the 2 channel CP correlation graph (Figure 7) it becomes apparant that at angles other than 45° the 2 channel CP is considerably stronger in the rejection of what should be non-matching images, particularly at 225°. This azimuth is where the targets are aligned spatially but in opposite directions. This effect is mainly due to the sole dependence on pixel intensity in the VV and RR comparisons, instead of the polarimetric dependence of the 2CP method.

The ability to reject incorrect targets is an important aspect for a target recognizer. The plots shown in Figures 8-10 were generated using a 45° aspect 5° elevation template of a T72M1 tank. The LP, CP, and 2CP cross correlations were calculated using T80U tank test images. The T80U and T72M1 tanks are very similar in their overall size and shape, making them likely candidates for a false alarm. The plots for LP and CP comparisons show some correlation at the matching 45° test angle, but the 2CP comparison shows virtually no correlation.

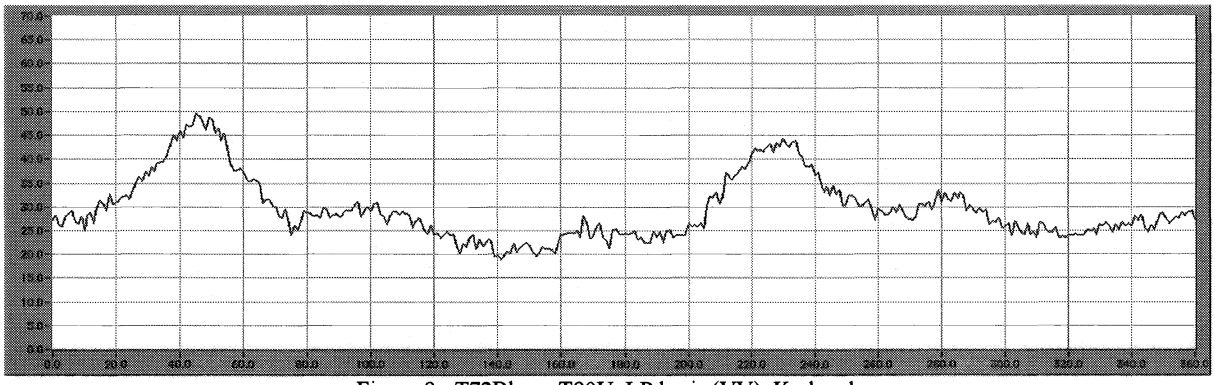

Figure 8: T72Bk vs. T80U, LP basis (VV), Ka-band.

Figure 9: T72Bk vs. T80U, CP basis (RR), Ka-band.

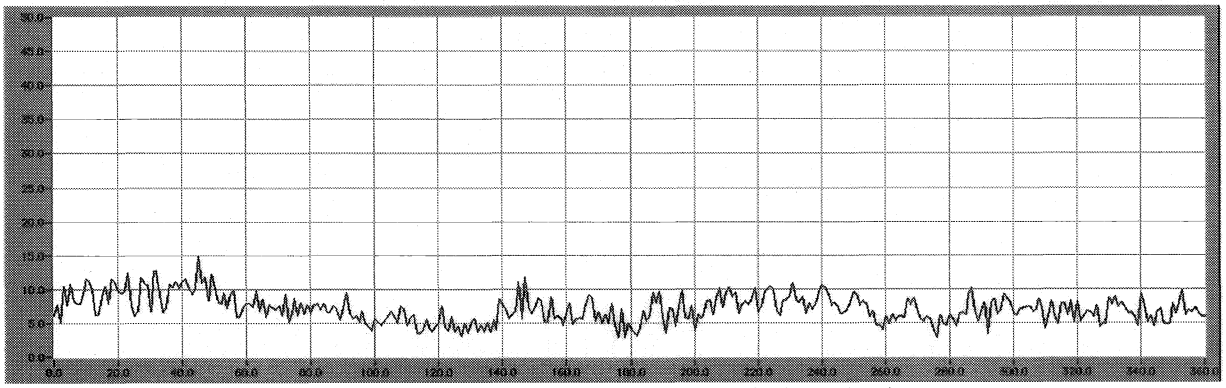

Figure 10: T72Bk vs. T80U, 2CP basis, Ka-band.

6.2 Comparisons

The study on Ka-band and W-band data sets had a number of variations of targets and target configurations. Tables 2a and 2b list the data and some details of the configurations.

Ka-band Data Sets

#	Tank type	Elevation angle	Turret position (degrees)	Description
1.	Challenger	5°	0°	
2.	T72Bk	5°	9°	Turntable off, barrels on
3.	T72Bk	5°	9°	Turntable on, barrels on
4.	T72Bk	5°	0°	Turntable off, barrels on
5.	T72Bk	5°	36°	Turntable off, barrels on
6.	T72Bk	5°	9°	Turntable off, barrels off
7.	T72M1	5°	0°	Vehicle #1
8.	T72M1	5°	0°	Vehicle #2
9.	T72M1	5°	0°	Vehicle #2
10.	T80U	5°	0°	

Table 2a: Ka-band data set descriptions.

W-band Data Sets

#	Tank type	Elevation angle	Turret position (degrees)	Description
1.	T80B	15°	0°	Ground plane
2.	Challenger	15°	0°	Ground plane
3.	Challenger	15°	0°	Ground plane, reprocessed data (#2)
4.	Challenger	15°	0°	Ground plane
5.	Challenger	15°	0°	Ground plane, reprocessed data (#4)
6.	Challenger	15°	30°	Ground plane
7.	Challenger	20°	30°	Ground plane
8.	T80B	15°	0°	Free space
9.	T55	15°	0°	
10.	M48	15°	0°	
11.	Leclerc	15°	0°	
12.	Leclerc	20°	0°	

Table 2b: W-band data set descriptions.

All of the data sets were compared within their own band using the LP, CP, and 2CP methods. Listed in the tables in Figures 11-16 are the peak scores experienced in the 35°-55°range (against a ~45° template) and the nearest false alarm (highest score in the 0°-34° and 56°-360° sets).

peak score 35°-55° / highest false alarm 0°-34°, 56°-360° Ka 1LP RESULTS

	1	2	3	4	5	6	7	8	9	10
1	100.0/									
2	46.2/45.1	100.0/								
3	44.9/46.1	69.0/48.3	100.0/							
4	47.9/45.7	67.8/51.3	66.3/50.2	100.0/						
5	44.3/45.2	63.4/48.0	61.1/49.4	67.2/48.5	100.0/					
6	45.0/46.6	73.2/49.3	67.7/49.6	68.2/53.0	67.9/49.2	100.0/				
7	46.7/44.5	54.6/48.5	53.6/48.4	53.6/49.4	52.0/44.0	53.1/47.0	100.0/			
8	45.2/42.3	56.2/46.5	56.3/48.6	53.5/44.9	53.9/47.4	58.3/46.3	57.2/47.5	100.0/		
9	45.1/44.0	55.9/46.2	56.1/47.9	53.3/45.6	53.8/46.0	57.5/45.5	57.0/48.0	83.3/45.1	100.0/	
10	46.7/41.6	52.2/45.6	53.4/45.9	54.9/43.4	53.6/45.6	54.1/46.9	49.8/45.7	50.7/43.4	49.4/44.4	100.0/

Figure 11: Results of the comparisons of the Ka-band data sets, done in LP (VV).

peak score 35°-55° / highest false alarm 0°-34°, 56°-360° Ka 1CP RESULTS

	1	2	3	4	5	6	7	8	9	10
1	100.0/									
2	40.1/39.4	100.0/								
3	41.7/41.4	66.8/46.0	100.0/							
4	41.7/41.8	65.7/49.8	64.2/50.0	100.0/						
5	40.3/42.4	64.0/44.0	58.8/44.3	65.2/43.5	100.0/					
6	42.0/43.0	70.1/45.0	66.4/46.2	67.0/49.3	67.4/44.6	100.0/				
7	42.0/40.0	50.0/43.4	51.9/42.3	48.0/43.6	49.3/41.7	49.7/45.1	100.0/			
8	40.0/34.8	49.0/39.2	51.0/41.0	48.3/40.2	46.3/39.5	49.8/42.1	57.3/44.7	100.0/		
9	40.4/38.2	50.3/41.1	53.6/40.4	49.7/42.2	48.0/40.1	51.5/42.3	58.9/46.0	79.4/41.2	100.0/	
10	43.4/34.5	46.1/40.0	47.7/41.9	48.0/41.1	46.6/40.3	47.1/40.0	46.1/41.6	44.1/41.2	44.2/41.5	100.0/

Figure 12: Results of the comparisons of the Ka-band data sets, done in CP (RR).

peak score 35°-55° / highest false alarm 0°-34°, 56°-360° Ka 2CP RESULTS

	1	2	3	4	5	6	7	8	9	10
1	100.0/									
2	18.2/15.7	100.0/								
3	17.7/18.7	32.4/16.8	100.0/							
4	18.8/16.4	32.6/20.9	29.8/19.6	100.0/						
5	17.4/18.9	32.4/16.7	25.2/18.3	39.3/17.2	100.0/					
6	18.8/17.2	41.4/15.6	31.3/18.3	36.8/24.5	42.3/20.4	100.0/				
7	16.2/13.8	16.9/14.5	18.4/17.5	18.9/15.9	18.0/14.9	18.2/16.3	100.0/			
8	13.9/12.1	20.1/17.1	20.4/16.2	18.6/15.5	17.9/15.2	20.5/16.5	27.3/18.8	100.0/		
9	16.8/14.4	17.3/14.5	21.2/16.7	21.4/15.1	19.6/17.4	20.0/17.1	28.9/21.1	53.1/16.3	100.0/	
10	16.7/17.0	19.4/15.3	18.3/13.6	18.2/15.4	16.2/13.8	18.2/15.2	14.3/13.0	15.5/12.6	14.7/12.7	100.0/

Figure 13: Results of the comparisons of the Ka-band data sets, done in 2CP.

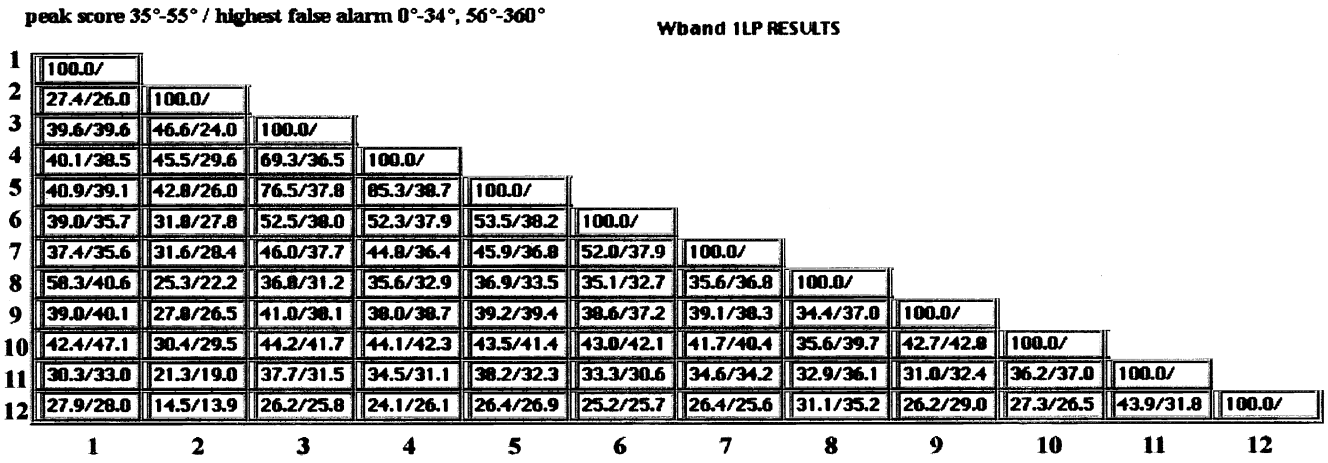

Figure 14: Results of the comparisons of the W-band data sets, done in LP (VV).

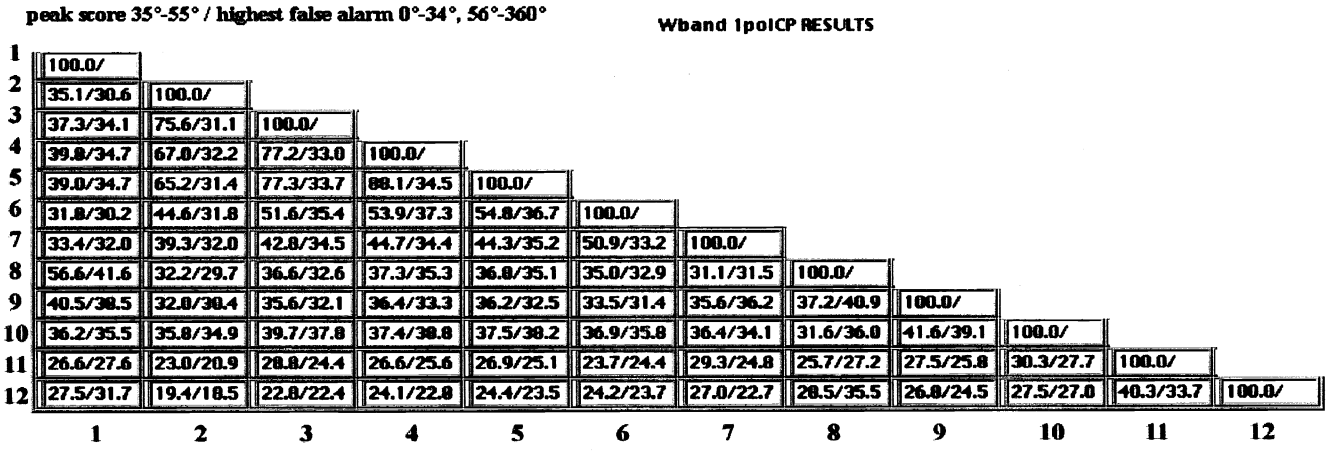

Figure 15: Results of the comparisons of the W-band data sets, done in CP (RR).

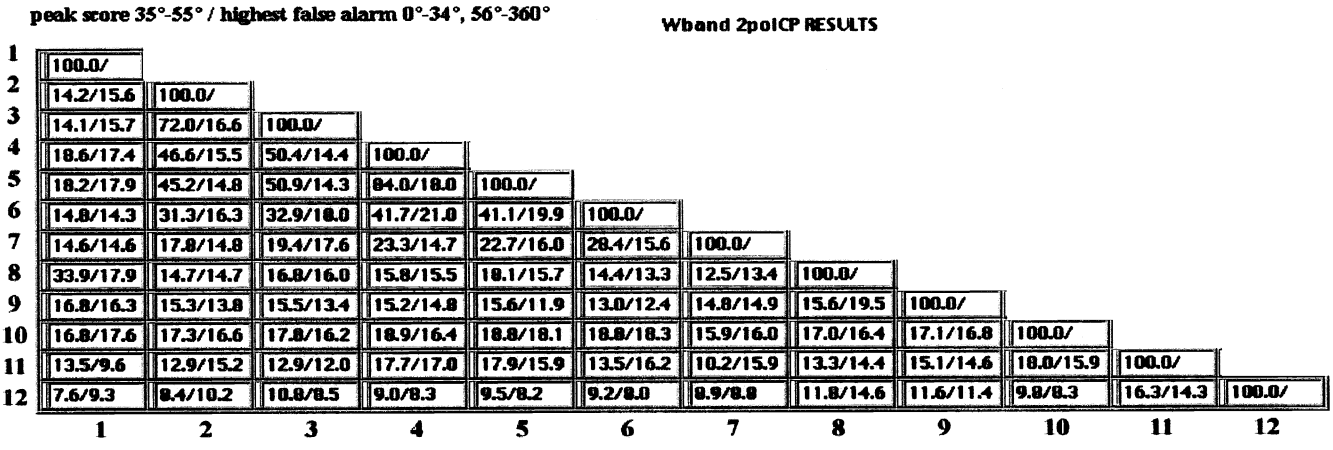

Figure 16: Results of the comparisons of the W-band data sets, done in 2CP.

A good target recognizer will match the proper targets and reject any other targets. Within the Ka-band sets, data runs 2-6 should match each other, data runs 7-9 should match each other, and all other combinations should be rejected. In the W-band data sets, data runs 1 and 8 should match each other, and data runs 2-6 should match each other. Data runs 2-6 may or may not match with data run 7, which is taken on the same target but at 20 degrees elevation, so it won't be a requirement, as with data runs 12 and 13. In total the 111 non-self comparisons should definitely yield 24 "matches" and 82 "rejects", with 6 comparisons (the 20 degree sets) undetermined.

If a simple peak score threshold is used to determine a "match" or a "reject", the 2CP method works flawlessly in both the Ka-band and W-band data sets with a 25% threshold. The LP comparisons do not. Using a threshold just high enough to avoid any false alarms (59% for Ka-band sets, 49% for W-band sets) the test does not recognize 6 out of the 24 matching targets. The CP comparisons do appear to be more consistent than the LP comparisons, missing 1 comparison out of the 24 with the threshold also set just high enough to avoid any false alarms (54% for Ka-band, 46% for W-band). Of particular interest was the LP method's inability to recognize the two different vehicles of the same type, T72M1s #1 and #2, in the Ka-band data sets. In order to set a threshold low enough to match these tanks, several false alarms are noted. The 2CP and the CP methods recognize these tanks with no false alarms. The template images for all of the comparisons shown in Figures 11-16 were always the 45° aspect images directly out of the data sets. Additional analysis not reported here indicates that the results are independent of the template aspect angle.

In overall performance the 2CP method is the most consistent for matching and rejecting targets. It is a bit of a surprise that the CP method outperformed the LP method, since the scoring plots (Figures 5-6, 8-9) appear so similar. Additional analysis should improve the performance of the 2CP method, given the considerably suppressed false alarm probability, but is beyond the scope of this study.

7. Conclusion

A simple yet effective polarimetric ATR is described in this report. First, the polarimetric behavior of scatterers over a varying look angle has been studied using a 3-D imaging system, scaling W-band radar. Based on these results odd/even bounce difference images (2CP) have been generated using two channels of circular polarization scale model ISAR data. These new images have been tested in a simple 2-D cross-correlation, and the results compared to similar correlations performed on simple single channel intensity images in LP and CP bases.

The 2CP method described in this report easily identifies different targets from the same class (i.e. a T72 tank from a T80 tank). In addition to basing the "scores" on polarimetric aspects of the target, the 2CP method reduces unresolvable scattering inherent in range/cross-range SAR image formation and its negative effect on any recognition scheme. The result is that spatial alignment of different targets of similar size and shape produces a very low 2CP correlation score compared to the cross-correlation score of two data runs of the same target.

Future research includes studies of additional different targets of the same type, and studies of full scale versus model data (ref. [5]). Initial results are promising for continued success in identifying full scale targets with model data templates using the 2CP method. This work will be described in a future report.

---

1. G. B. De Martinis., "Design of a Coherent Polarimetric 1.56 THz Receiver for Three Dimensional Radar Imaging of Scaled Model Targets", Masters Thesis, University of Massachusetts Lowell.
2. G. B. De Martinis, T. M. Goyette, M. Coulombe, J. Waldman, **"a 1.56 THz Spot Scanning radar Range for Fully Polarimetric W-Band Scale Model Measurements"**, Proceedings of the 22nd Annual Symposium of the Antenna Measurements and Techniques Association, October 2000 Philadelphia, PA.
3. T. M. Goyette, J. C. Dickinson, J. Waldman, and W. E. Nixon, **"1.56 THz Compact Radar Range for W-Band Imagery of Tactical Targets"**, Proc. SPIE **4053**, p 615, April 2000 Orlando FL.
4. T.M. Goyette, J. C. Dickinson, J. Waldman, W. E. Nixon, and S. Carter, **"Fully Polarimetric W-band ISAR Imagery of Scale-Model Tactical Targets Using a 1.56 THz Compact Range"**, Proc. SPIE **4382** April 2001 Orlando FL (to be published).
5. R. H. Giles, **"Study of Target Variability and Exact Signature Reproduction Requirements for Ka-Band Radar Data"**, SPIE **4380** April 2001 Orlando FL (to be published).